

Two-mode frequency-stabilised He-Ne (633 nm) lasers: studies of short- and long-term stability

To cite this article: P E Ciddor and R M Duffy 1983 *J. Phys. E: Sci. Instrum.* **16** 1223

View the [article online](#) for updates and enhancements.

Related content

- [Control of laser frequencies using a Fabry-Perot interferometer and DAC techniques](#)
B Stahlberg
- [Laser frequency stability measurement using a Fabry-Perot based system](#)
B S Gray, S P Spoor and I D Latimer
- [Frequency stability measurement on magnetic Lamb dip-stabilised lasers](#)
M Oger, A Daude and A Le Floch

Recent citations

- [Method of improving the frequency repeatability of the intensity stabilized HeNe laser](#)
Grzegorz Budzy *et al*
- [Frequency Noise Properties of Lasers for Interferometry in Nanometrology](#)
Jan Hrabina *et al*
- [Frequency stabilization of an internal mirror He-Ne laser with a high frequency reproducibility](#)
Xiaofei Diao *et al*

Two-mode frequency-stabilised He-Ne (633 nm) lasers: studies of short- and long-term stability

P E Ciddor and R M Duffy

CSIRO Division of Applied Physics, Sydney, Australia 2070

Received 23 May 1983

Abstract. This paper discusses the practical design and performance of lasers stabilised by balancing the powers in two orthogonally polarised modes. Procedures for aligning the optical system and for optimising the electronic controller are described. The performances of several types of commercial tubes have been tested over periods of over three years. A short-term (1 s) stability of 20 kHz and a long-term (several months) stability of 10 MHz have been achieved with some tubes. An additional characteristic of these lasers is their good power stability (within 0.1% over several hours).

1. Introduction

The frequency stabilisation of a two-mode He-Ne laser at 633 nm was first reported by Balhorn *et al* (1972). Developments of the technique, in which the power in the two modes is balanced, have been described by Bennett *et al* (1973), Desai *et al* (1979), Gordon and Jacobs (1974), and Yoshino (1980), and there are several commercial instruments based on it. Most of the published work was aimed at very modest stabilities over short times, typically 4 parts in 10^8 over several hours, although Balhorn *et al* (1975a) monitored the wavelength over several years, and are currently monitoring the frequencies of a group of lasers (private communication).

Our objective was to develop a laser that combined ease of operation with a short-term stability of a few parts in 10^{10} , to allow frequency comparison with an iodine-stabilised laser, and a stability over several months of a few parts in 10^8 , which is comparable with that of a ^{86}Kr lamp. Such lasers are convenient alternatives to iodine-stabilised lasers in routine length metrology. This paper describes the construction and adjustment of our lasers and presents results obtained over several years for several types of laser tubes. The optical, thermal and electronic requirements are outlined.

There are several other techniques for stabilising lasers which give comparable stability: Morris *et al* (1975) used mode collapse in a transverse-Zeeman laser, Tobias *et al* (1965) balanced the powers of the two modes in a longitudinal-Zeeman laser, and Baer *et al* (1980) balanced the frequency-offset in a similar laser. These techniques are relatively complicated, as they require magnetic fields, complex electronics, and in some cases, modifications to the laser tube itself.

2. Optical and mechanical design

We adopted a DC control system so as to keep the optical and electronic components as simple as possible. Other workers have favoured choppers (Desai *et al* 1979) or polarisation modulators (Yoshino 1980) in conjunction with a single detector, with the intention of eliminating slow drifts in the controlled frequencies.

Our experience leads us to believe that the drift of modern

operational amplifiers is negligible, and that both long- and short-term stability can be maintained more easily if rotating or vibrating components are avoided. We use a 45° calcite Wollaston prism (see figure 1) which separates the polarised components of the weak back beam by 20° , and two large PIN photodiodes (Siemens Type BPW34, active area $2.75 \text{ mm} \times 2.75 \text{ mm}$). The laser is tuned by a bifilar heater coil wound directly on the laser tube and cemented in place with an epoxy varnish. The response time of this simple thermal control has proved to be short enough, though faster alternatives have been described by Magyar (1979) and Baer *et al* (1980). The laser tube is supported on Nylon adjusting screws within a rigid cage. The ballast resistor is enclosed in a glass sleeve within the cage, and the whole assembly (laser, prism and photodiodes) is housed in a brass tube that is blackened inside and out. The heat load on the assembly is made up of about 10 W from the discharge, 2 W from the ballast, and 2 W from the heater; it results in a temperature of about 70°C at the surface of the laser tube. This is rather close to the recommended limits, and it might be preferable to provide gentle convective cooling by means of fins or a vented enclosure. Yoshino (1980) used a fan instead of a heater; this lowers the temperature, but may reduce the short-term stability.

The first step in the optical alignment of the system is to adjust the prism and the photodiodes so that the polarised beams fall centrally on them. It is essential to avoid feedback to the laser from surface reflections (Brown 1981). For this reason, the prism should be tilted by a few degrees relative to the beam from the laser. The diodes are mounted directly on a circuit board that is normal to the optical axis; this ensures that they are each at about 10° to the laser beams. Larger tilts are undesirable because they produce reflection losses and possible asymmetry in the detected signals.

The second step is to adjust the tube in its mount so that the orthogonal polarisation directions of the modes are parallel to the axes of the Wollaston prism. This is done most accurately by setting a polariser to extinguish one output of the Wollaston prism, and then transferring the polariser to the main output beam from the laser. The output beam is then observed with an optical spectrum analyser, and the laser tube is rotated until only a single longitudinal mode is shown by the analyser. Contrary to the assertion by Yoshino (1980), the accuracy required is quite low ($10\text{--}20^\circ$), because the sensitivity of the servo control is proportional to $\cos 2\theta$, where θ is the angle of misalignment.

If a spectrum analyser is not available, a satisfactory alignment can be achieved by observing the differential output from the photodiode amplifier as the tube warms up, and rotating the tube until the peak-to-peak signal is greatest. Care is needed during the adjustment to ensure that the beams remain centred on the photodiodes.

3. Electronic design

The circuit is shown in figure 1. The power available in the back beam of a typical 2 mW laser is $10\text{--}50 \mu\text{W}$ in each polarisation. In the servo mode, the heater power is controlled by the imbalance between the photodiode currents. The reversing switch determines whether the balance condition corresponds to the frequency of the horizontally polarised mode being higher or lower than that of the vertically polarised mode. Initially, the heater is driven at full power and IC1 is connected as a comparator, thus producing alternations in the sign of its output, which is fed to the auto-lock circuit. Positive-going transitions of this signal are sharpened by the switch T2-T3, and the period of alternation is compared with that of a timer, IC2. As thermal equilibrium is approached the period exceeds that of the timer, which trips off. Switch S then closes the feedback loop around IC1 and connects the heater to its output

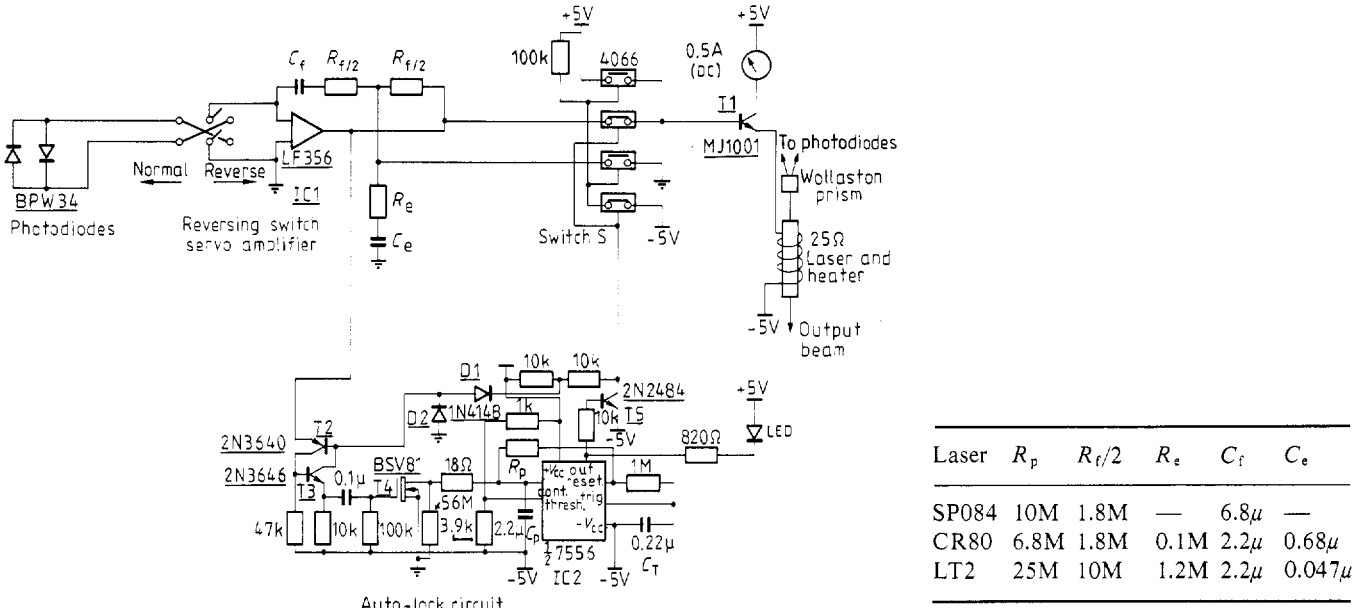


Figure 1. Circuit diagram of frequency controller and auto-lock circuit.

via T1. Further triggering of the timer by noise pulses is prevented by T5 and D1, which inhibit the switch T2-T3 until power is removed and C_T is fully discharged. The period of the timer is set by $R_p C_p$; a typical value is 30 s. The laser and its enclosure form a complex thermal circuit, and phase compensation may be required to prevent oscillation, depending on the characteristics of the particular laser. The design of the compensating network, and the selection of suitable time constants for the integrator are outlined in Appendix I. The overall gain in the feedback system is about 10^6 for frequencies below 0.01 Hz. Faster fluctuations, due to changes in the ambient temperature, are damped by the thermal inertia of the laser. We have found it important to have indications of abnormally high or low heater current, and of the presence of optical feedback. These indications are most conveniently provided by a meter that displays the heater current, which is usually about 250 mA. Low heater current indicates that the servo has locked before the laser assembly has reached thermal equilibrium. High heater current occurs if the auto-locking process has been repeatedly defeated by mechanical shock or optical feedback. Optical feedback usually affects one polarised beam more than the other and therefore introduces a frequency offset. This offset fluctuates rapidly as thermal or acoustic changes occur in the external optical path. The corresponding fluctuations in heater current are easily seen on the meter, and, in addition, they are filtered and used to modulate a panel lamp to alert the operator to the problem. In extreme cases the feedback may drive the servo out of lock.

4. Frequency offsets

Ideally, the control system would force the laser to operate at two frequencies symmetrically disposed about the centre of the gain curve. In practice, the operating condition is that in which the input to the integrator is nearly zero. We can calculate the actual operating frequencies on the basis of the following assumptions.

- (i) The power curve is gaussian, with a half width equal to a .
- (ii) The mode separation $\Delta\nu$ may take different values, $\Delta\nu_1$ or $\Delta\nu_2$, depending on whether the horizontally or vertically polarised mode is higher in frequency (Balhorn *et al* 1975b).

(iii) The overall response S_V of the detector to vertically polarised light is related to that for horizontally polarised light S_H , by $S_V = S_H(1 + \varepsilon)$, where ε is small. S_V and S_H include the peak power of the laser in each polarisation, the transmittance of the prism, and the sensitivities of the photodiodes.

(iv) The integrator has an input offset current equivalent to a small fraction (η) of the response to vertically polarised light at the balance condition.

These assumptions lead to the following equation for balance of the servo system:

$$\exp[-(\nu_H - \nu_0)/a]^2 = (1 + \varepsilon)(1 + \eta) \exp[-(\nu_V - \nu_0)/a]^2. \quad (1)$$

This equation can be solved for the operating frequencies ν_V , ν_H by using the assumption that ε and η are small.

We find that there are four possible operating frequencies

$$\nu_{1H} = \nu_0 + \Delta\nu_1/2 - (a^2/2\Delta\nu_1)(\varepsilon + \eta) \quad (2)$$

$$\nu_{1V} = \nu_{1H} - \Delta\nu_1 \quad (3)$$

$$\nu_{2H} = \nu_0 - \Delta\nu_2/2 + (a^2/2\Delta\nu_2)(\varepsilon + \eta) \quad (4)$$

$$\nu_{2V} = \nu_{2H} + \Delta\nu_2, \quad (5)$$

where ν_0 is the line-centre frequency.

The first pair corresponds to one polarity of the photodiode connection, and the second pair is obtained by reversing the connections of the photodiodes to the integrator. The availability of four slightly different frequencies can be advantageous in practical measurements, as was pointed out by Balhorn *et al* (1975a). An effective frequency which is almost independent of the setting of the control system is obtained by taking the mean:

$$\bar{\nu} = \frac{1}{4}(\nu_{1H} + \nu_{1V} + \nu_{2H} + \nu_{2V}) = \nu_0 + \frac{1}{4}(a^2/\Delta\nu^2)(\Delta\nu_2 - \Delta\nu_1)(\varepsilon + \eta) \quad (6)$$

where $\Delta\nu = (\Delta\nu_1 \Delta\nu_2)^{1/2}$.

We have found differences between the four operating frequencies of 1 to 50 MHz, depending on the alignment of the laser and the selection of the diodes (which vary by about 5% in sensitivity). The input offset of a good FET input operational amplifier is easily made less than 200 pA, whereas the photodiode signals are of the order of 5 μ A, so η is about

4×10^{-5} and may be neglected. For a typical He-Ne laser, $\Delta\nu$ is about 600 MHz and a is 720 MHz, so that $a^2/2\Delta\nu_1 \approx 430$ MHz. We infer that ε is usually in the range 0.01–0.02, and $\bar{\nu}$ should be within 0.1 MHz of ν_0 . In practice larger variations in $\bar{\nu}$ occur, because of drifts in frequency over the settling time of the controller operation of the reversing switch (see figure 1).

The value of any one of the four available frequencies, say ν_{1H} in equation (2) would be expected to depend slightly on the temperature at which control is achieved, because the frequency interval $\Delta\nu$ depends on the length of the laser cavity. The change in length required to reproduce a given sequence of polarisations (VH in this case) is one wavelength, corresponding to a temperature change of about 1 K for a 2 mW borosilicate glass plasma tube. The change in ν_{1H} would then be only about 1.5 kHz. In practice larger changes in frequency are observed, as reported later in this paper. In normal operation, a stability of 1 part in 10^8 corresponds to a temperature stability of about 3 mK.

5. Results

All frequency measurements were made by comparison with a laser stabilised by saturated absorption in $^{129}\text{I}_2$, having a short-term stability and a reproducibility of about 4 parts in 10^{11} (20 kHz) (Magyar and Brown 1980). We studied one or more samples of each of the following types of tube: Spectra-Physics SP084-1, Coherent CR80-2T, and Aerotech LT2R (two types of construction).

The most satisfactory tube was the SP084-1, but unfortunately later production versions exhibited intermittent transverse modes which made it impossible for the servo to maintain a steady state. This type of tube is no longer available, but it provides a benchmark against which the performance of other tubes may be tested. The CR80-2T tubes, which have an aluminium envelope, are less stable over short periods (seconds and minutes) than are the glass tubes. This may be due in part to the higher coefficient of linear expansion of the metal, but we also noticed that these tubes were extremely sensitive to optical feedback, which suggests that the transmittance of the output mirror is relatively high. We also tested a Tropel Model 100 laser system, which contains a CR80-2T tube and a stabilisation system similar to our own, with similar results.

In LT2R tubes the capillary extended beyond the coaxial envelope and the back mirror was mounted on this extension of the capillary. These tubes, and the CR80-2T tubes, which have a similar hybrid structure, exhibited an unexpected variation of frequency with ambient temperature, as described in Appendix II. These tubes also showed an oscillatory response to a step change in the control signal, which indicated that the transfer function of the equivalent thermal circuit was at least of third order. Current versions of the LT2R tube are coaxial throughout their length, like the SP084-1, and no temperature coefficient has been detected. However, these tubes exhibit cyclic variations of frequency of up to 30 MHz with a period of about 1 h.

The short-term stability of our lasers was determined by a computer-controlled Allan variance measuring system (Magyar and Brown 1980). The short-term stability is highly dependent on the amount of optical feedback, which was reduced by a polarisation isolator and low-reflectance beam-steering mirrors. The results shown in table 1 were not all obtained under ideal conditions, but they indicate what can be achieved fairly easily in practice. Under very carefully controlled conditions the Allan variance for 1 s or 10 s samples is comparable with that of the reference laser.

Table 2 shows data over longer periods, including some cases where the laser was moved around the building, or even

Table 1. Root Allan variance (σ) versus sampling time (τ) for various types of laser.

Tube	$\sigma(1\text{ s})$ (kHz)	$\sigma(10\text{ s})$ (kHz)	$\sigma(100\text{ s})$ (kHz)	$\sigma(1000\text{ s})$ (kHz)
SP084-1	30	30	66	200
CR80-2T	60	150	200	—
LT2R (old design)	55	50	130	150
LT2R (new design)	100	100	200	—
Tropel 100	80	220	390	—

Table 2. Long-term stability (reference frequency: component k of $^{129}\text{I}_2$).

Tube	Time (d)	Max. (MHz)	Min. (MHz)	Range (MHz)	Range (parts in 10^8)
SP084-1	1198	k-418	k-425	7	1.5
CR80-2T	29	k-424	k-481	57	12
LT2R (old)	213	k-214	k-226	12	2.5
Tropel 100	1065	k-84	k-136	52	10

carried by road for several hundred kilometres between measurements. Most of these measurements were of just one of the four possible frequencies discussed earlier, so that some of the observed variation may be due to slight changes in optical alignment, diode sensitivity, etc, which would average out over the four possible frequencies.

A useful secondary property of a laser stabilised in this way is its good power stability. We have found that the power in each mode shows peak-to-peak variations of about 0.1% in a bandwidth of 20 kHz, and is constant to about 0.1% over periods of several hours, as measured on a chart recorder with a response time of 1 s. This characteristic, which follows directly from the frequency stability, has been applied in an interferometer in which conventional modulation of the optical path was impracticable, but from which a sensitivity of 0.001 fringe was required. A slow radiometric scan of the static fringe pattern allowed the identification of the fringe peak to the required precision (Fisher *et al* 1980).

6. Conclusion

We have shown that the simple optical and electronic systems described above can provide a frequency stability of a few parts in 10^8 over long periods. The requirements for optimum performance are:

- (a) the use of a fully coaxial laser tube, or the use of a compensating heater or a temperature-stabilised enclosure for tubes that exhibit the behaviour described in Appendices I and II;
- (b) the absence of any transverse modes;
- (c) the minimisation of optical feedback;
- (d) the matching of the response of the integrating amplifier to the thermal response of the laser tube.

Acknowledgments

We thank N Brown for constructing the reference laser and much of the frequency-calibration equipment, and for discussions on the effects of optical feedback. The prototype mechanical assembly was designed and built by C H Freund. R Caffin of the CSIRO Division of Textile Physics kindly lent us the Tropel Model 100 laser.

Appendix I: Equivalent circuit for thermal analysis

Our initial thermal model assumed radial flow of heat from the discharge through the capillary, and thence through the brass tube to the atmosphere. Heat input to the heater around the envelope was also assumed to flow radially inwards and outwards.

The thermal circuit and its electrical equivalent are shown in figure 2(a) and (b). The contribution of the heater to the temperature of the laser envelope, which determines the frequencies of the laser modes, is given by the product of the heater power W and the thermal impedance Z presented by the entire structure. From figure 2(b) we derive

$$Z(p) = \frac{\tau_g q_g (\tau_{la} q_a + 1)}{p C_l \tau_g q_g (\tau_{la} q_a + 1) + p C_g (\tau_{la} q_a + 1) + C_a q_a \tau_g q_g}$$

$$q_i = p + 1/\tau_i \quad (i = a, g, la),$$

$p = j\omega$ is the complex circular frequency, $\tau_g = R_g C_g$ is the time constant for heat flow inwards, $\tau_{la} = R_l C_a$ is the time constant for heat flow to the outer cover, $\tau_a = R_a C_a$ is the time constant for heat flow from the cover to the ambient air, and

$$\tau_l = R_l C_l.$$

We assume that R_l , which is the thermal resistance of the static air between the laser tube and the outer cover, is larger than the other resistances, and that all the thermal capacitances are comparable. It follows that τ_l and τ_{la} are larger than all the other time constants. After some algebraic manipulation Z can be approximated by

$$Z(p) = \frac{p + 1/\tau_g}{C_l (p + \gamma/\tau_g)(p + 1/\gamma\tau_l)}$$

where $\gamma = 1 + C_g/C_l$.

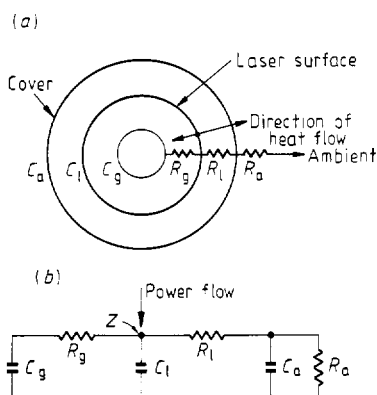


Figure 2. (a) Thermal model of the laser tube and its enclosure. (b) Equivalent circuit.

A Bode plot, calculated for reasonable values of various thermal parameters ($R_l = 5.8 \text{ K W}^{-1}$, $C_l = 24 \text{ J K}^{-1}$, $\gamma = 3.3$, $\tau_l = 139 \text{ s}$) is shown in figure 3. The feedback amplifier (figure 1) should behave as an integrator at low frequencies to maintain long-term laser frequency stability. However, at frequencies above γ/τ_g , where the phase shift due to the integrator and thermal delays approaches 180° , the system would become unstable. The feedback resistor R_f (figure 1) removes the 90° phase shift of the integrator at frequencies above $1/R_f C_f$, while the circuit acts as an integrator down to frequencies of $1/KR_l C_f$ where R_l is the back resistance of the parallel photodetectors, and K is the DC gain of the amplifier. Below this frequency the

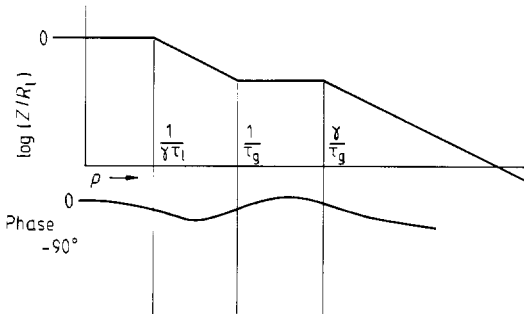


Figure 3. Bode plot of simplified equivalent circuit.

transimpedance of the circuit is KR_l . For the values of the parameters given earlier, $\gamma\tau_l = 460 \text{ s}$. We have found that time constants as short as 8 s for $R_f C_f$ give stable operation, provided the open-loop gain of the control system is high. The open-loop gain depends on the laser power, diode sensitivity, the thermal coefficient of expansion of the cavity, the gains of the operational amplifier and power amplifier and the shape of the laser power output curve at the operating frequencies. A typical value is 10^6 .

The oscillatory response with a period of about 1 s found with some tubes, as mentioned in the main text, seems to arise from an additional time delay along the capillary extension on which one mirror was mounted. Two methods were used to eliminate this. One was to wind a heater onto the capillary extension and to supply the same power per unit area to it as to the main tube; this minimised the temperature gradient and hence the heat flow and its attendant phase shift. The second, and simpler, method was to add components R_e and C_e (figure 1). Over the circular frequency range $4/R_f C_e$ to $1/R_e C_e$, the transimpedance of the circuit increases from R_f to $R_f^2/4R_e$ and the resulting phase advance has a maximum value at the geometric mean of these two frequencies. This geometric mean frequency is made the same as the oscillatory frequency, and for a maximum phase advance of 45° , the two frequencies are about a decade apart. Under these conditions

$$R_e = R_f/40$$

and

$$R_f/C_e = 12.6/\omega_r,$$

ω_r being the oscillatory circular frequency of the control system.

Even in the absence of such an oscillatory response, we have found that R_f should be kept below about $20 \text{ M}\Omega$ to avoid pick-up from the mains. We find typical values of 50 Hz noise across the heater to be 0.2 V peak-to-peak, and the wideband noise to be about 0.5 V peak-to-peak.

Appendix II: Sensitivity of some tubes to ambient temperature

As mentioned in the main text, we found that for certain types of laser tube the stabilised frequency depended on the ambient temperature. We made extensive tests on the optical and electronic components of our controllers without finding any temperature dependence of the necessary magnitude. We found that the temperature sensitivity vanished if the laser was controlled by the main output beam, rather than by the weak beam from the back mirror (the gain of the controller was reduced to compensate for the higher power). This implied that the source of the problem was in the transmittance of the back mirror, since any other property of the laser (reflectance or phase change at either mirror, misalignment of the capillary,

pressure or current changes) would have affected the behaviour when the front beam was used to control the frequency. It is well known (Yoshino 1972, Keijser 1977, Bouchiat and Pottier 1981) that laser mirrors exhibit birefringence, but the values quoted are typically phase differences of a few milliradians.

We suggest the following mechanism for the observed behaviour. The back mirror of these tubes is mounted on an extension of the main capillary, and is some distance from the heater. It is therefore cooler than the main structure of the laser, and its temperature is also more likely to follow changes in the ambient temperature. The transmittance (T) of a highly reflecting multilayer stack is determined mostly by surface scattering, which is expected to be anisotropic because of residual polishing patterns on the substrate and anisotropic structure in the multilayer coating. A very slight change in the amount of this anisotropy will have a significant effect on the difference signal sensed by the controller, and will cause the controller to retune the laser. Alternatively, a slight bending of the capillary extension would move a different area of the multilayer into the beam, so any lateral variation in the anisotropy would produce a similar result. Either of these effects will change the relative sensitivity ($1 + \varepsilon$) in the two channels of the controller. The magnitude of $d\varepsilon/dT$ required to account for the observed variation of about 20 MHz K⁻¹ is found from equation (2) to be about 0.03 K⁻¹. If we assume that the reflectance (R) and absorptance (A) are isotropic but that the scattering (Σ) is anisotropic, we can express the contribution of the anisotropy to ε in the form

$$\varepsilon = (T_V - T_H)/T_V = (\Sigma_H - \Sigma_V)/T_V.$$

Highly reflecting multilayer coatings have typical parameters

$$T \approx 0.003, \quad \Sigma_H \approx \Sigma_V \approx 0.001,$$

so

$$\varepsilon \approx 300(\Sigma_H - \Sigma_V)$$

$$\delta\varepsilon \approx 300\delta(\Sigma_H - \Sigma_V).$$

The observed value $d\varepsilon/dT = 0.03 \text{ K}^{-1}$ would be accounted for by

$$d(\Sigma_H - \Sigma_V)/dT = 1 \times 10^{-4} \text{ K}^{-1},$$

that is, if the anisotropy varied by 10% of the scattering coefficient per degree. If the anisotropy itself were small, say 10%, this would represent a doubling for a 1 K change in temperature. This is unlikely but a variation of this amount caused by variations in anisotropy across the mirror is conceivable.

The abnormal behaviour of these tubes was eliminated, as described in Appendix I, by providing an additional heater to bring the entire laser tube to a uniform temperature. Alternative solutions would be to enclose the entire system in a temperature-controlled enclosure (Desai *et al* 1979), or to sample the main beam. The latter solution would be difficult to implement without introducing a large imbalance in the polarised components, and hence a large frequency offset. Such a large offset has been deliberately generated by Puntambekar *et al* (1982); it might be expected to vary significantly with the laser power.

References

- Baer T, Kowalski F V and Hall J L 1980 Frequency stabilization of a 0.633 μm He–Ne longitudinal Zeeman laser *Appl. Opt.* **19** 3173
- Balhorn R, Kunzmann H and Lebowsky F 1972 Frequency stabilization of internal-mirror helium–neon lasers *Appl. Opt.* **11** 742–4
- Balhorn R, Lebowsky F and Ullrich D 1975a *Berichte Leistungsfähigkeit der Frequenzstabilisierung von He–Ne-Lasern nach dem Zwei-Moden-Vergleichsverfahren* (Braunschweig: Physikalisch-Technische-Bundesanstalt)
- Balhorn R, Lebowsky F and Ullrich D 1975b Beat frequency between two axial modes of a He–Ne laser with internal mirrors and its dependence on cavity Q *Appl. Opt.* **14** 2955–9
- Bennett S J, Ward R E and Wilson D C 1973 Comments on: frequency stabilization of internal mirror He–Ne lasers *Appl. Opt.* **12** 1406
- Bouchiat M A and Pottier L 1981 A high-purity circular polarization modulator: application to birefringence and circular dichroism measurements on multielectric mirrors *Opt. Commun.* **37** 229–33
- Brown N 1981 Frequency stabilized lasers: optical feedback effects *Appl. Opt.* **20** 3711–4
- Desai J N, Chandrasekhar T and Madhavan R 1979 Frequency stabilisation of He–Ne lasers *J. Phys. E: Sci. Instrum.* **12** 1040–2
- Fisher L R, Parker N S and Sharples F 1980 An interference method for measurement of thickness variations in thin liquid films *Opt. Engng.* **19** 834–8
- Gordon S K and Jacobs S F 1974 Modification of inexpensive multimode lasers to produce a stabilized single frequency beam *Appl. Opt.* **13** 231
- Keijser R A J 1977 Polarization properties of internal mirror He–Ne lasers in a strong transverse magnetic field *Opt. Commun.* **23** 194–8
- Magyar J A 1979 A simple rapid thermal length control for lasers and etalons *J. Phys. E: Sci. Instrum.* **11** 647–8
- Magyar J A and Brown N 1980 High resolution saturated absorption spectra of iodine molecules ¹²⁹I₂, ¹²⁹I¹²⁷I, and ¹²⁷I₂ at 633 nm *Metrologia* **16** 63–8
- Morris R H, Ferguson J B and Warniak J S 1975 Frequency stabilization of internal mirror He–Ne lasers in a transverse magnetic field *Appl. Opt.* **14** 2808
- Puntambekar P N, Dahiya H S and Chitnis V T 1982 Frequency stabilized and tunable multimode He–Ne lasers *Opt. Commun.* **42** 60
- Tobias I, Skolnick M L, Wallace R A and Polanyi T G 1965 Derivation of a frequency-sensitive signal from a gas laser in an axial magnetic field *Appl. Phys. Lett.* **6** 198–200
- Yoshino T 1972 Polarization properties of internal-mirror He–Ne lasers at 6328 Å *Japan J. Appl. Phys.* **11** 263
- Yoshino T 1980 Frequency stabilization of internal-mirror He–Ne ($\lambda = 633 \text{ nm}$) lasers using the polarization properties *Japan J. Appl. Phys.* **19** 2181